Durham DTP/96/38
MPI-PhT/96-28
April, 1996

Perturbative description of particle spectra at LEP-1.5

VALERY A. KHOZE[1,2,3] * , SERGIO LUPIA[3] † , WOLFGANG OCHS[3] ‡

[1] *Department of Physics*
University of Durham, Durham DH1 3LE, UK

[2] *Institute for Nuclear Physics*
St. Petersburg, Gatchina, 188350, Russia

[3] *Max-Planck-Institut für Physik*
Werner-Heisenberg-Institut
Föhringer Ring 6, D-80805 Munich, Germany

Abstract

The recent data from LEP-1.5 on charged particle spectra are analyzed within the analytical QCD approach.

*e-mail: v.a.khoze@durham.ac.uk
†e-mail: lupia@mppmu.mpg.de
‡e-mail: wwo@mppmu.mpg.de

1. Introduction

e^+e^- annihilation into hadrons proves to be a wonderful laboratory for detailed experimental tests of QCD. The high statistics data collected from hadronic Z^0 decays in LEP-1 and SLD experiments [1] allow one to perform detailed studies of perturbative QCD and to reduce the domain of our ignorance on the physics of confinement. The data have convincingly demonstrated the dominant role of the perturbative phase of jet evolution and supported the hypothesis of local parton-hadron duality [2,3]. We have now quite successfully entered the stage of quantitative tests of the so-called Modified Leading Log Approximation (MLLA) which allows one to calculate systematically the inclusive jet characteristics up to terms of relative order $\sqrt{\alpha_s}$ [3,4,5]. In some special cases next-to-MLLA corrections are also calculated, (for reviews see [6,3,7]).

In November 1995 LEP was operated at centre-of-mass energies 130-140 GeV (LEP-1.5). The first experimental data [8,9,10,11] show good agreement with perturbative expectations. In particular, semihard QCD results have become available now.

Further studies of the various aspects of QCD dynamics will be provided by LEP-2 and future linear e^+e^- colliders (for discussion, see e.g. [12] and [13]) as well as by HERA and TEVATRON. It is worthwhile to mention the unique opportunity to compare the particle spectra measured by the same experimental group at the same accelerator at different energies.

The aim of this paper is twofold. First of all we would like to perform the complete analysis of the recent data on inclusive charged particle distributions collected by LEP-1.5. We show that the inclusive charged particle spectra and mean multiplicity agree impressively well with the analytical QCD results. Secondly we would like to discuss the working tools relevant for the detailed treatment of the forthcoming data.

2. Inclusive charged particle spectrum in QCD jets

In the MLLA this spectrum can be obtained as solution of the appropriate evolution equation [3,4] in terms of two parameters, the QCD scale Λ and the $k_\perp$ cut-off Q_0 in the cascade. In the case when both parameters coincide ($Q_0 = \Lambda$) one obtains the so-called limiting parton spectrum [6,14] which has been proven to be very successful in fitting the experimental data of charge particle production in QCD jets.

Until now, characteristics of an individual quark jet have been studied in greatest detail experimentally in the reaction $e^+e^- \to$ hadrons. An inclusive momentum spectrum here is the sum of two q-jet distributions. In terms of the limiting spectrum one obtains for the distribution in the variable $\xi = \log 1/x$ with $x = 2E_h/\sqrt{s}$

$$\frac{1}{\sigma}\,\frac{d\sigma^h}{d\xi} \;=\; 2K^h D_q^{\lim}(\xi, Y) \qquad (1)$$

where K^h is the hadronization constant, $\sqrt{s}$ the total *cms* energy and $Y = \log(\sqrt{s}/2\Lambda)$. The limiting spectrum is readily given using an integral representation for the confluent hypergeometric function [4,3]:

$$D_q^{\lim}(\xi, Y) \;=\; \frac{4C_F}{b}\,\Gamma(B)\int_{-\frac{\pi}{2}}^{\frac{\pi}{2}}\frac{d\ell}{\pi}\,e^{-B\alpha}\left[\frac{\cosh\,\alpha + (1-2\zeta)\sinh\,\alpha}{\frac{4N_C}{b}\,Y\,\frac{\alpha}{\sinh\,\alpha}}\right]^{B/2}$$

$$\times\, I_B \left(\sqrt{\frac{16N_C}{b}\, Y\, \frac{\alpha}{\sinh\,\alpha}\, [\cosh\,\alpha + (1-2\zeta)\,\sinh\,\alpha]} \right). \tag{2}$$

Here $\alpha = \alpha_0 + i\ell$ and α_0 is determined by $\tanh\,\alpha_0 = 2\zeta - 1$ with $\zeta = 1 - \frac{\xi}{Y}$. I_B is the modified Bessel function of order B, where $B = a/b$, $a = 11N_C/3 + 2n_f/3N_C^2$, $b = (11N_C - 2n_f)/3$, with n_f the number of flavours and $C_F = (N_C^2 - 1)/2N_C = 4/3$.

The analysis of charged particle spectra using this distribution [15,16,17] yields values for the effective scale parameter $\Lambda \equiv \Lambda_{ch}$ in the range $\Lambda_{ch} \simeq 250 \div 270$ MeV. If both parameters Q_0 and Λ are kept free in the fit one recovers the limiting spectrum with $Q_0 = \Lambda$ as best solution [17].

It proves to be very convenient (see e.g. [18,14,17]) to analyze inclusive particle spectra in terms of the normalized moments

$$\xi_q \equiv < \xi^q > = \frac{1}{\bar{\mathcal{N}}_E} \int d\xi \xi^q D(\xi) \tag{3}$$

where $\bar{\mathcal{N}}_E$ is the mean multiplicity in the jet, the integral of the spectrum. These moments characterize the shape of the distribution and are independent of normalization uncertainties. The theoretical predictions for the moments from the Limiting Spectrum are determined by only one free parameter Λ_{ch}. Also one defines the cumulant moments $K_q(Y,\lambda)$ or the reduced cumulants $k_q \equiv K_q/\sigma^q$ [19] which are related by

$$\begin{aligned}
K_1 &\equiv \overline{\xi} \equiv \xi_1 \\
K_2 &\equiv \sigma^2 = < (\xi - \overline{\xi})^2 >, \\
K_3 &\equiv s\sigma^3 = < (\xi - \overline{\xi})^3 >, \\
K_4 &\equiv k\sigma^4 = < (\xi - \overline{\xi})^4 > - 3\sigma^4
\end{aligned} \tag{4}$$

where the third and fourth reduced cumulant moments are the skewness s and the kurtosis k of the distribution. If the higher-order cumulants ($q > 2$) are sufficiently small, one can reconstruct the ξ-distribution from the distorted Gaussian formula, see [18].

The cumulant moments can be obtained from [18]

$$K_q(Y,\lambda) = \int_0^Y dy \left(-\frac{\partial}{\partial\omega} \right)^p \gamma_\omega(\alpha_s(y)) \Big|_{\omega=0} \tag{5}$$

where $\gamma_\omega(\alpha_s(y))$ denotes the anomalous dimension which governs the energy evolution of the Laplace transform $D_\omega(Y)$ of the ξ-distribution $D(\xi, Y)$. Equation (5) shows the direct dependence of the moments on $\alpha_s(Y)$ and thereby implicitly on n_f.

The analytical procedure of [14] allows one to arrive at the following expression for the moments:

$$\bar{\mathcal{N}}_{LS} = \Gamma(B) \left(\frac{z}{2}\right)^{1-B} I_{B+1}(z) \tag{6}$$

$$\frac{< \xi^q >}{Y^q} = P_0^{(q)}(B+1, B+2, z) + \frac{2}{z}\frac{I_{B+2}(z)}{I_{B+1}(z)} P_1^{(q)}(B+1, B+2, z) \tag{7}$$

where the parameter B is introduced above and the variable z is given by $z \equiv \sqrt{16N_cY/b}$; $P_0^{(q)}$ and $P_1^{(q)}$ are polynomials of order $2(q-1)$ in z. Explicit results for the full expressions for $q < 3$ can be found in [14] and for $q = 3,4$ in [20].

In the calculations, the partons were taken massless and the p_t cut-off $Q_0 \equiv \Lambda_{ch}$ was introduced for regularization; on the other hand, the observable hadrons are massive. One can make the simple assumption that the cut-off Q_0 is related to the masses of hadrons. As a first stage in the discussion of charged particle spectra, one can relate Q_0 to an effective hadron mass, then for both partons and hadrons $E \geq Q_0$. A consistent kinematical behaviour of parton and hadron spectra can be obtained through the relation [17]:

$$E_h \frac{dn(\xi_E)}{dp_h} = E_p \frac{dn(\xi_E)}{dp_p} \quad ; \quad E_h = E_p \geq Q_0 \tag{8}$$

at the same energies E_i or $\xi_{E_i} = \log(\sqrt{s}/2E_i)$ (not momentum!), where $E_h = \sqrt{p_h^2 + Q_0^2}$ and $E_p = p_p$. With this choice both spectra vanish linearly for $E \to Q_0$ or $\xi_E \to Y$.

3. Comparison with data

LEP-1.5 opens a unique opportunity to compare the high energy data collected at the same accelerator by the same Collaboration§. Later on such a comparison will be continued at LEP-2.

Momentum spectrum

Figure 1a shows experimental data on charged particle inclusive momentum distributions, $dn/d\xi_p$ as a function of $\xi_p = \log(\sqrt{s}/2p)$, obtained by the OPAL Collaboration at *cms* energies $\sqrt{s} = 91.2$ GeV (LEP-1) [15] and $\sqrt{s} = 133$ GeV (LEP-1.5) [11]. Theoretical predictions of the Limiting Spectrum (2) at the same *cms* energies are also shown; at both *cms* energies, the Λ_{ch} parameter has been taken equal to 270 MeV, as suggested by the moment analysis performed in [17], whereas the free overall normalization factor has been fixed to the value $K^h = 1.31$¶. In view of the forthcoming run at LEP-2, theoretical predictions for $\sqrt{s} = 200$ GeV with the same choice of parameters are also shown. In Figure 1b data on inclusive momentum distributions extracted at LEP-1.5 *cms* energy by different experimental Collaborations, i.e., ALEPH [8], DELPHI [9]‖ and OPAL [11] are compared to the same theoretical predictions as in Figure 1a. The Limiting Spectrum predictions with this choice of parameters reproduce very well the experimental shape around the peak at LEP-1 *cms* energy; the agreement at LEP-1.5 is reasonable, even though deviations are visible in the region around the maximum. However, this effect

§at lower energies such a comparison has been performed by TASSO Collaboration at PETRA [21].

¶OPAL Collaboration [15] found a best value of $\Lambda_{ch} = 253$ MeV at LEP-1 with $K_h = 1.28$ from a fit to the shape, whereas $\Lambda_{ch} = 263 \pm 4$ MeV was obtained from a fit to the peak position by using the asymptotic formula[11]. The value for $\Lambda_{ch} = 270$ MeV has been chosen in [17] to reproduce the moments over a large energy interval. With a restriction to the LEP-1 data, a smaller value of Λ_{ch} would fit slightly better.

‖DELPHI published the charged particle inclusive energy distribution obtained by assigning to all particles the pion mass. The inclusive momentum distribution has been extracted from experimental data by using the same assignment to the mass of all particles.

could be well attributed to statistical and/or systematic uncertainties, as suggested by the large spread of experimental points shown in Figure 1b.

Looking first at the large x_p (small ξ_p) region, the experimental data can be well described at both *cms* energies by the Limiting Spectrum prediction (1), contrary to the simple distorted Gaussian parametrization (not shown). The observed agreement of the Limiting Spectrum prediction in a kinematical region where the MLLA approach is not expected *a priori* to be valid is due to the fact that the approximate expression for the anomalous dimension derived within MLLA at small x_p turns out to mimic reasonably well the expression valid at large x_p (see [22,16,23] for more details).

In the small x_p (large ξ_p) region, data show a tail which is not well reproduced by theoretical predictions taking ξ_p as an argument in (2). This discrepancy is actually due to kinematical effects [16,17]. As previously discussed, theoretical predictions vanish for $E < Q_0$, i.e., for $\xi_E > Y$. This kinematical effect can be taken into account in a simple way by using the relation (8) between parton and hadron spectra. The corresponding theoretical predictions for the spectrum can then be written as:

$$\frac{1}{\sigma}\frac{d\sigma^h}{d\xi_p} = 2K^h \frac{p}{E} D_q^{\lim}(\xi_E, Y) \qquad , \qquad \xi_E = \log \frac{\sqrt{s}}{2\sqrt{se^{-2\xi_p}/4 + Q_0^2}} \tag{9}$$

For $E \gg Q_0$ these differences vanish and $dn/d\xi_p \simeq dn/d\xi_E$, $\xi_E \simeq \xi_p$. It is seen in Figures 1a and 1b (dashed lines) that they closely follow the large ξ tail of the experimental data. The best fit here is obtained with $K^h = 1.34$. It is also worth noticing that a common normalization factor, K^h, has been used at both *cms* energies; this result is consistent with the expectations of LPHD.

Moments

The moments $< \xi^q >$ and the cumulants K_q are determined from the spectra Edn/dp as a function of ξ_E; the average multiplicity $\bar{\mathcal{N}}_E$ is obtained as the integral over ξ_E of the full spectrum Edn/dp. For the unmeasured interval near $\xi_E \simeq Y$ (small momenta) a contribution was found by linear extrapolation as in Notice that $\bar{\mathcal{N}}_E$ coincides with the usual particle multiplicity, $\bar{\mathcal{N}}$, the integral over ξ_p, at asymptotic energies. At LEP-1 (LEP-1.5) the difference is about 10% (8%)**. The cumulants up to order q=4 together with the corresponding MLLA predictions at *cms* energy $\sqrt{s} = 133$ GeV are shown in Table 1. Notice that DELPHI has also presented data at the Z^0 peak from radiative events collected at LEP-1.5. Cumulants extracted from different experiments are consistent within experimental uncertainties; it is important to stress that also radiative events at the Z^0 peak collected at LEP-1.5 are completely consistent with LEP-1 results. Errors quoted in the Table are statistical errors only. Note that moments of order $q \geq 1$ are independent of the overall normalization, which is the main source of systematic uncertainties. On the other hand, a systematic error of the order of 0.5 should be taken into account for the average multiplicity at LEP-1.5 energy. Also shown in the Table are the results [17] obtained at LEP-1 for comparison. Theoretical predictions are shown for the Limiting Spectrum with $\Lambda_{ch} = 270$ MeV; for the average multiplicity $\bar{\mathcal{N}}_E$ the first number in the Table refers to the prediction (6) normalized at LEP-1, the second number to the extrapolation of the fit $\bar{\mathcal{N}}_E = c_1 \frac{4}{9} 2\bar{\mathcal{N}}_{LS} + c_2$ to the energy region 3-91 GeV [17]. The

**Good fits have been obtained also for the standard charged particle multiplicity, $\bar{\mathcal{N}}$ [8,9,10,11].

agreement between experimental results and theoretical predictions is very satisfactory; the deviation visible in the prediction of the average multiplicity at LEP-1.5 is well inside the errors if one correctly takes into account systematics.

Peak position

An easily accessable characteristic of the ξ-distribution is its maximum ξ^* which has been extensively studied by the experimental groups (for a recent review, see e.g. [24]). The high energy behaviour of this quantity for the Limiting Spectrum is predicted as [14,22]:

$$\xi^* \;=\; Y\,\left[\frac{1}{2}\;+\;\sqrt{\frac{C}{Y}}\;-\;\frac{C}{Y}\right] \tag{10}$$

with the constant term given by

$$C \;=\; \frac{a^2}{16\,N_C b} \;=\; 0.2915\;(0.3513)\;\text{for}\;n_f \;=\; 3(5).$$

Alternatively, one can compute the maximum ξ^* from the Distorted Gaussian approximation:

$$\xi^* = \overline{\xi} - \frac{1}{2} s\,\sigma \tag{11}$$

using the full expression (7) for the moments defined in (4). One neglects here the contribution of cumulants of order greater than 4 to the position of the maximum. The third possibility is to extract numerically the actual position of the maximum ξ^* from the Limiting Spectrum (2); the comparison between the three choices can give us some information on the validity of the approximations performed in the first two cases. A comparison of these three possible approaches is shown in Figure 2a for $n_f = 3$. Notice that since we are plotting ξ^* vs. Y, there is no dependence of theoretical predictions on Λ_{ch}.

One can conclude from Figure 2a that the energy dependence of the maximum ξ^*, i.e., the slope of the curve, is very similar in the three cases; a finite shift, however, is present; for example the true maximum of the Limiting Spectrum ξ^* can be expressed in terms of the approximation (10) as:

$$\xi^* \;=\; Y\,\left[\frac{1}{2}\;+\;\sqrt{\frac{C}{Y}}\;-\;\frac{C}{Y}\right] + 0.10 \tag{12}$$

(The numerical term actually decreases slightly from 0.11 at $\sqrt{s} = 10$ GeV to 0.086 at 130 GeV).

In Figure 2b we compare experimental data on the maximum ξ^* extracted from Gaussian or Distorted Gaussian fits†† to the central region of the inclusive momentum spectrum [21,25,26,27,28,29,30,31,32,15,8,11] with the theoretical predictions obtained extracting the maximum from the shape of the Limiting Spectrum. We found a good agreement for $\Lambda_{ch} = 270$ MeV, which also describes the energy evolution of the moments. The best value of Λ_{ch} which fits the experimental data is slightly different, depending

††We used the ξ^* values from the original publications or from the fits[24].

on which theoretical formula is beeing used. For instance, by using the asymptotic formula (12), a smaller value of Λ_{ch} would have been better. The difference in the Λ_{ch} value is of the order of 20-30 MeV.

Another possible source of ambiguity is the number of active flavours to be used in the theoretical formula. This problem can be studied most easily[17] for the moments of the ξ-distribution whose evolution with energy follows from (5). In this formula the number of flavours enters through the running coupling $\alpha_s(y, n_f)$. The moments evolve at low energy with 3 active flavours and with 4 and 5 flavours after passing continuously the respective thresholds. As the MLLA is based on the one-loop expression for α_s there remains a scale ambiguity. The simplest approach would be to put the thresholds at the heavy quark masses, i.e., to set the scale of running α_s to $\frac{\sqrt{s}}{2}$. However, let us remind that α_s depends on the transverse momentum k_t and kinematics forces $k_t \leq \frac{1}{4}\frac{\sqrt{s}}{2}$. This would suggest to move the thresholds to 4 m_Q or towards even larger values, since the effective value of k_t would be in general smaller than the maximum allowed value. Taking the presence of heavier flavours into account in this way, one finds small deviations at LEP-1 energies in the higher moments $q \geq 2$ [17]. However, for ξ^* using the approximation (11) the effect of the higher flavours is only of the order of 1% and taking $n_f = 3$ is a very good approximation. This is demonstrated in Table 2 which compares the predictions for ξ^* under different assumptions on the flavour composition and effective thresholds.

There is also a small difference between the maximum ξ^* of the Limiting Spectrum (2) and the modified distribution (9) by about 1%. This dependence may be considered as systematic uncertainty of the predictions.

Let us also point the attention to the fact that the prediction of the Limiting Spectrum (11) describes the data quite well without the need of any additional constant contribution which might be due to the hadronization process.

4. Conclusions

The analysis of the recent LEP-1.5 data demonstrates that the analytical perturbative description of inclusive particle distributions in QCD jets is in a quite healthy shape. The charged particle spectrum (up to the overall normalization) and the moments with $q \geq 1$ as well as their energy dependence can be described with only one adjustable scale parameter Λ_{ch}. For these observables, no additional sizeable effects from hadronization are visible. The present data allow one to observe even relatively small effects caused by higher order terms. Finally, let us emphasize that in our view it is quite impressive that even a limited sample of hadronic events (corresponding to integrated luminosity of about 5 pb^{-1}) allows one to perform so good tests of the perturbative picture of multiple hadroproduction in jets. Having in mind the prospects of QCD studies at LEP-2, this looks rather promising.

5. Acknowledgements

We thank P. Abreu, G. Cowan, L. Del Pozo and G. Dissertori for useful discussions of the experimental data. The work was supported in part by the UK Particle Physics and

Astronomy Research Council.

References

[1] For reviews of the latest results at Z^0 see, e.g.
A. De Angelis, J. Fuster, W. Metzger, R. Settles, T. Maruyama, N. Watson and F. Verbeure, talks at 1995 Int. Europhysics Conference on High Energy Physics, 27 July – 2 Aug. 1995, Brussels, Belgium.

[2] Ya. I. Azimov, Yu. L. Dokshitzer, V. A. Khoze and S. I. Troyan, Z. Phys. C27 (1985) 65; ibid., C31 (1986) 213.

[3] Yu.L. Dokshitzer, V.A. Khoze, A.H. Mueller, S.I. Troyan, Basics of Perturbative QCD, (Editions Frontières, Gif-sur-Yvette CEDEX-France, 1991).

[4] Yu. L. Dokshitzer and S. I. Troyan, Proc. 19th Winter School of the LNPI, Vol. 1, p.144; Leningrad preprint LNPI-922 (1984).

[5] A. H. Mueller, Nucl. Phys. B213 (1983) 85; Erratum quoted ibid., B241 (1984) 141.

[6] Yu. L. Dokshitzer, V. A. Khoze, A. H. Mueller and S. I. Troyan, Rev. Mod. Phys. 60 (1988) 373.

[7] V. A. Khoze and W. Ochs, “Perturbative QCD approach to multiparticle production”, preprint Durham DTP/96/36, MPI-PhT-96/29 (1996).

[8] ALEPH Coll., D. Buskulic et al., CERN preprint CERN-PPE/96-43, March 1996, submitted to Phys. Lett. B.

[9] DELPHI Coll., P. Abreu et al., Phys. Lett. B372 (1996) 172.

[10] L3 Coll., M. Acciarri et al., Phys. Lett. B371 (1996) 137.

[11] OPAL Coll., M. Z. Akrawy et al., CERN preprint CERN-PPE/96-47, March 1996, submitted to Z. Phys. C.

[12] V. A. Khoze, in Proceedings of the XXIXth Rencontre de Moriond, Méribel, France, March 1994, ed. J. Tran Thanh Van, Editions Frontiéres, 19 – 26 March, p.57;
P. Nason, B.R. Webber et al., “QCD”, Proceedings of the Workshop at LEP-2, Eds. G. Altarelli, T. Sjöstrand and F. Zwirner, CERN Report 96-01, Vol. 1, p. 249, 1996.

[13] V. A. Khoze, in Proceedings of the Workshop “Physics and Experiments with e^+e^- Linear Colliders”, Saariselkä, Finland, 1991, eds. R. Orava, P. Eerola and M. Nordberg (World Scientific, Singapore, 1992), p.547.

[14] Yu. L. Dokshitzer, V. A. Khoze and S. I. Troyan, Int. J. Mod. Phys. A7 (1992) 1875.

[15] OPAL Coll., M. Z. Akrawy et al., Phys. Lett. B247 (1990) 617.

[16] Yu. L. Dokshitzer, V. A. Khoze and S. I. Troyan, Z. Phys. C55 (1992) 107.

[17] S. Lupia and W. Ochs, Phys. Lett. B365 (1996) 339.

[18] C. P. Fong and B. R. Webber, Phys. Lett. B229 (1989) 289; Nucl. Phys. B355 (1991) 54.

[19] A. Stuart and J. K. Ord, Kendall's Advanced Theory of Statistics, v.1, (Griffin, London, 1987), p.107.

[20] S. Lupia and W. Ochs, contributed paper EPS 0803 to 1995 Int. Europhysics Conference on High Energy Physics, 27 July – 2 August 1995, Brussels, Belgium, and paper in preparation.

[21] TASSO Coll., W. Braunschweig et al., Z. Phys. C47 (1990) 187

[22] Yu. L. Dokshitzer, V. A. Khoze and S. I. Troyan, J. Phys. G17 (1991) 1481; 1602.

[23] V. A. Khoze, Yu. L. Dokshitzer and S. I. Troyan, Proceedings of the 20th Int. Symposium on Multiparticle Dynamics, Gut Holmecke near Dortmund, Germany, Sept. 1990, eds. R. Baier and D. Wegener (World Scientific, 1991), p.288.

[24] M. Schmelling, Physica Scripta 51 (1995) 683.

[25] MARK II Collaboration, A. Peterson et al., Phys. Rev. D37 (1988) 1.

[26] TPC/2γ Collaboration, H. Aihara et al., Phys. Rev. Lett., 61 (1988) 1263.

[27] CELLO Collaboration, H.J. Behrend et al., Phys. Lett. B256 (1991) 97;
O. Podobrin, Ph.D. thesis Univ. Hamburg, "Studies of Multihadron Final States in Electron Positron Annihilation", Report DESY FCE-92-03 (1992).

[28] AMY Collaboration, H. Aihara et al., Y. K. Li et al., Phys. Rev. D41 (1990) 2675.

[29] TOPAZ Collaboration, R. Itoh et al., Phys. Lett. B345 (1995) 335.

[30] ALEPH Coll., D. Buskulic et al., Z. Phys. C55 (1992) 209.

[31] DELPHI Coll., P. Abreu et al., Phys. Lett. B347 (1995) 447.

[32] L3 Coll., B. Adeva et al., Phys. Lett. B259 (1991) 199.

6. Figure Caption

Figure 1. **a.** Charged particle inclusive momentum distributions at $\sqrt{s} = 91.2$ GeV (LEP-1) [15] (diamonds) and $\sqrt{s} = 133$ GeV (LEP-1.5) [11] (triangles) as measured by the OPAL Collaboration in comparison with theoretical predictions of the Limiting Spectrum with $\Lambda_{ch} = 270$ MeV (solid line). Dashed lines show the predictions of the Limiting Spectrum after correction for kinematical effects. Theoretical predictions are also shown for $\sqrt{s} = 200$ GeV.
b. Charged particle inclusive momentum distribution at $\sqrt{s} = 133$ GeV (LEP-1.5) measured by ALEPH [8] (diamonds), DELPHI [9] (squares) and OPAL Collaborations [11] (triangles), and compared to the same theoretical curves as in **a**.

Figure 2. **a.** Maximum of the inclusive momentum distribution ξ^* as a function of $Y = \log \frac{\sqrt{s}}{2\Lambda_{ch}}$; comparison between different theoretical predictions: maximum numerically extracted from the shape of the Limiting Spectrum (solid line), asymptotic formula (10) (dashed line), eq. (11) (dotted line).
b. Maximum of the inclusive momentum distribution ξ^* as a function of $Y = \log \frac{\sqrt{s}}{2\Lambda_{ch}}$; comparison between experimental data (see text) and theoretical prediction numerically extracted from the shape of the Limiting Spectrum (solid line); $\Lambda_{ch} = 270$ MeV. Crosses are put at *cms* energies $\sqrt{s} = 200$ GeV and 500 GeV.

7. Table Caption

Table 1. The average multiplicity $\bar{\mathcal{N}}_E$, the average value $\bar{\xi}_E$, the dispersion σ^2, the skewness s and the kurtosis k of charged particles' energy spectra Edn/dp as a function of ξ_E with $\Lambda_{ch} = 270$ MeV extracted from experimental data at *cms* energies $\sqrt{s} = 91.2$ GeV and 133 GeV. In brackets the theoretical predictions of the Limiting Spectrum; the second entry in the average multiplicity column contains the results of the two parameter formula $\bar{\mathcal{N}}_E = c_1 \frac{4}{9} 2\bar{\mathcal{N}}_{LS} + c_2$; the first one the fit with $c_2 = 0$.

Table 2. Dependence on the number of active flavours of the theoretical prediction (11) for the maximum of the inclusive momentum spectrum. Results at three different *cms* energies are shown.

Table 1

Exp.	$\sqrt{s}$ (GeV)	$\bar{\mathcal{N}}_E$	$\bar{\xi}_E$	σ^2	s	k
ALEPH [30]	91.2	18.81±1.05	3.24±0.04	0.99±0.05	-0.39±0.10	-0.59±0.32
DELPHI [31]	91.2	19.17±1.00	3.32±0.02	1.03±0.01	-0.40±0.02	-0.59±0.07
L3 [32]	91.2	18.74±1.09	3.28±0.06	0.99±0.06	-0.35±0.13	-0.65±0.40
OPAL [15]	91.2	18.95±1.00	3.29±0.01	0.99±0.01	-0.36±0.03	-0.59±0.09
LEP-1 (avg)	91.2	18.93±0.52	3.29±0.01	1.01±0.02	-0.39±0.02	-0.59±0.05
DELPHI–γ [9]	91.2	19.20±0.20	3.33±0.04	0.99±0.03	-0.46±0.05	-0.44±0.18
MLLA	91.2	(input,input)	(3.27)	(1.00)	(-0.35)	(-0.52)
ALEPH [8]	133	22.04±0.35	3.52±0.06	1.19±0.04	-0.37±0.07	-0.62±0.26
DELPHI [9]	133	22.27±0.31	3.47±0.05	1.13±0.05	-0.40±0.08	-0.49±0.29
OPAL [11]	133	21.50±0.38	3.51±0.07	1.19±0.04	-0.35±0.07	-0.63±0.25
MLLA	133	(22.6,22.5)	(3.50)	(1.14)	(-0.34)	(-0.52)

Table 2

	ξ^*		
n_f	$\sqrt{s} = 29$ GeV	$\sqrt{s} = 91$ GeV	$\sqrt{s} = 133$ GeV
3	2.725	3.447	3.683
5	2.789	3.525	3.764
thresholds at m_Q	2.746	3.482	3.721
thresholds at 4 m_Q	2.729	3.463	3.703
thresholds at 8 m_Q	2.726	3.455	3.695

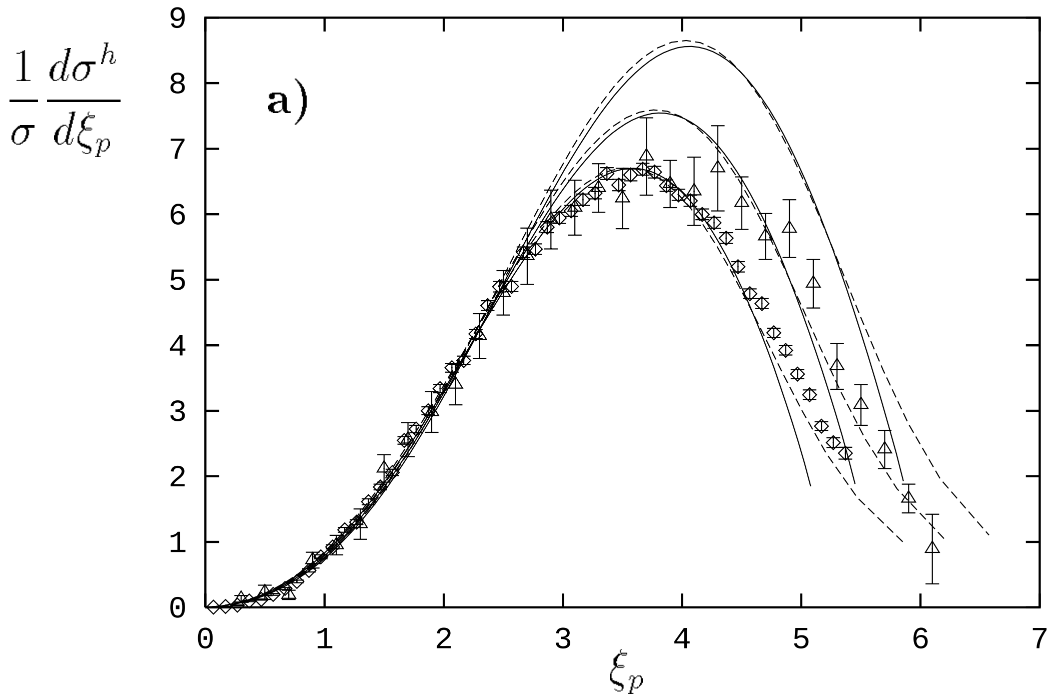
$\frac{1}{\sigma}\frac{d\sigma^h}{d\xi_p}$
a)
0
1
2
3
4
5
6
7
8
9
0
1
2
3
4
5
6
7
ξ_p

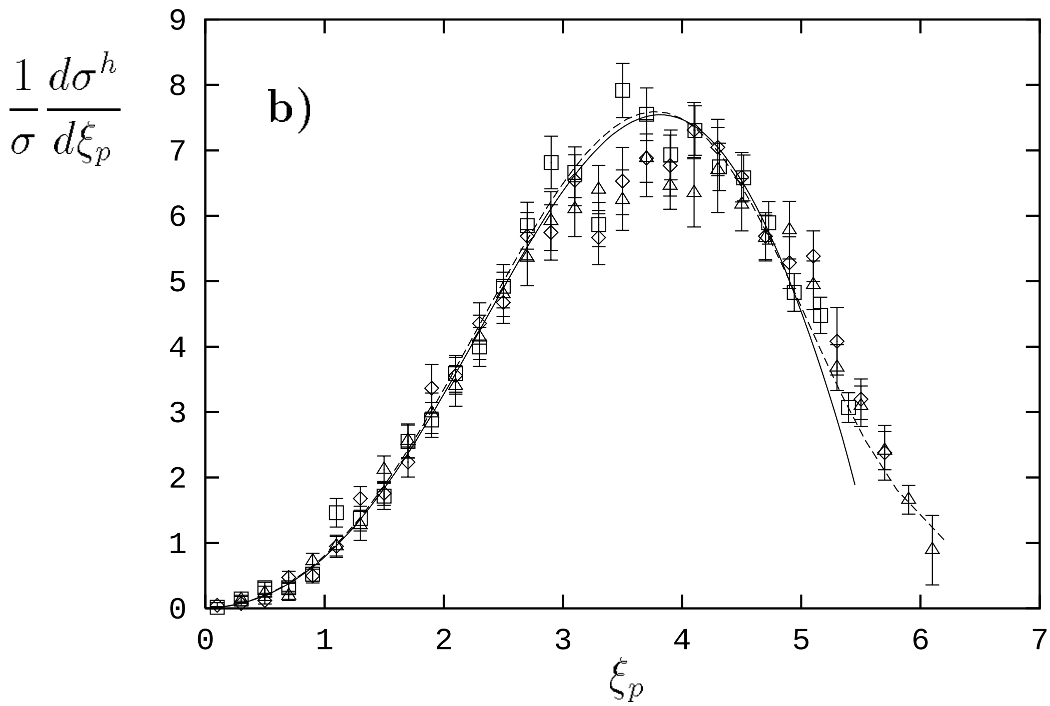
$\frac{1}{\sigma}\frac{d\sigma^h}{d\xi_p}$
b)
0
1
2
3
4
5
6
7
8
9
0
1
2
3
4
5
6
7
ξ_p

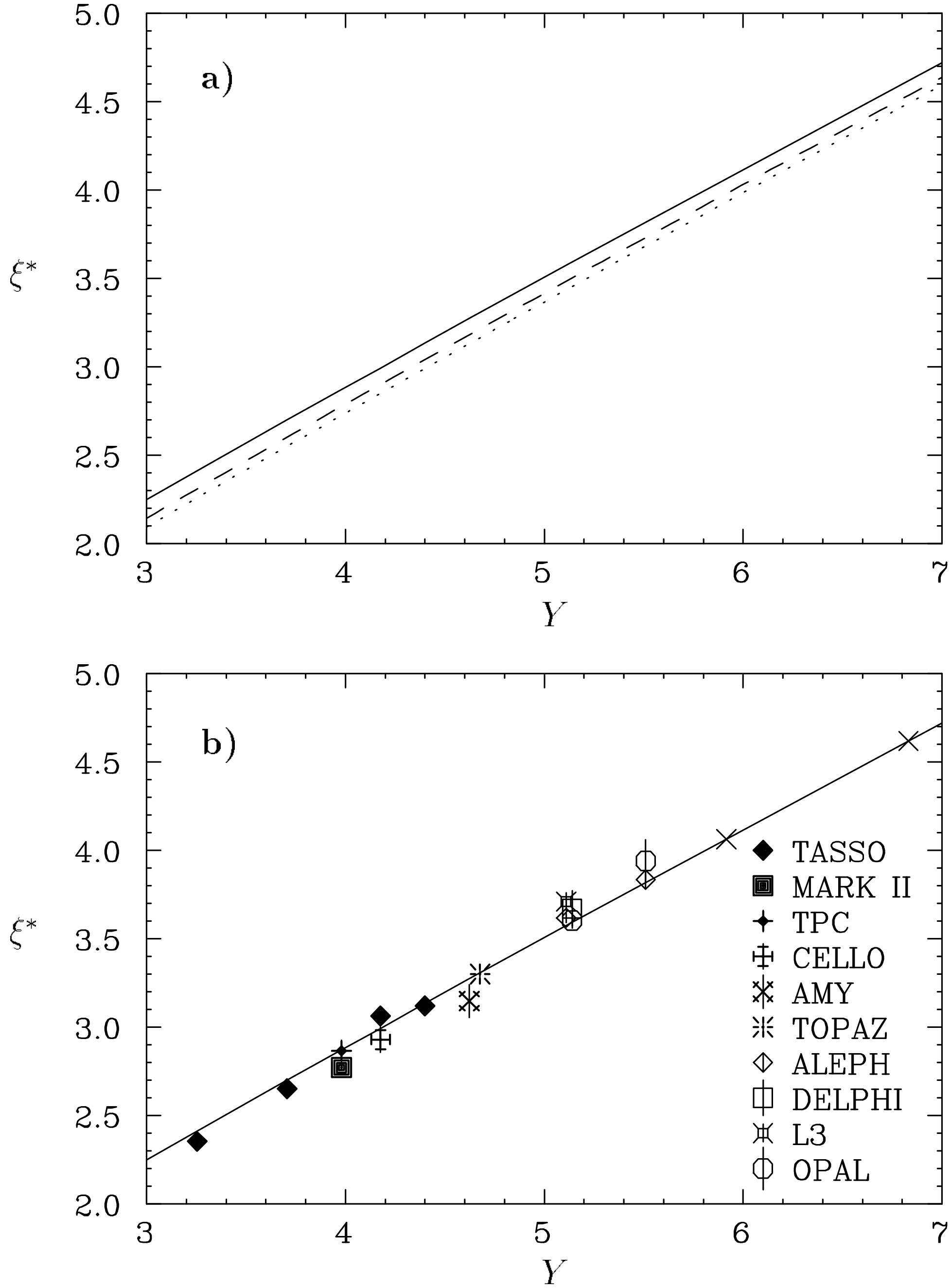
a)
ξ^*
Y
5.0
4.5
4.0
3.5
3.0
2.5
2.0
3
4
5
6
7
b)
TASSO
MARK II
TPC
CELLO
AMY
TOPAZ
ALEPH
DELPHI
L3
OPAL